Evaluation of miniature specimens for the determination of low constraint cleavage toughness

A H Sherry[1], S Jacques[1], M A Wilkes[1], G Wardle[1] and P J Budden[2]

[1] Serco Assurance, Risley, Warrington, WA3 6AT, UK.
[2] British Energy Generation Ltd, Barnwood, Gloucester, GL4 3RS, UK.

ABSTRACT: *This paper presents a feasibility programme undertaken to assess the potential for using pre-cracked Charpy V-notch (PC-CVN) specimens to measure low constraint toughness properties in the cleavage fracture regime. The approach adopted is to use a modified PC-CVN specimen to create a low constraint shallow-cracked three-point bend specimen. The specimen is prepared by fatigue pre-cracking a short 1mm crack from the V-notch, and subsequently removing the upper 2mm of the specimen (including the notch). The resulting specimen has a width of 8mm, a thickness of 10mm and a crack length to specimen width ratio of 0.125. Tests have confirmed that this geometry is suitable for generating low constraint toughness data in the lower transition regime. The data provide useful validation for the constraint-based methods in the R6 procedure.*

INTRODUCTION

In recent years, a considerable body of evidence has been published regarding the influence of crack-tip constraint on fracture toughness. High constraint configurations, such as deeply cracked geometries loaded in bending, generate high levels of stress triaxiality ahead of the crack tip. Conversely, low constraint configurations, such as shallow cracked geometries loaded in tension, generate a weaker triaxial stress field ahead of the crack tip. Experimental studies have demonstrated that a reduction in constraint leads to an effective increase in toughness. Two parameter (J-Q) fracture mechanics has been developed to quantify the influence of crack-tip constraint on fracture in the elastic-plastic regime. Here Q is defined by [1]:

$$\sigma_{ij} = \sigma_{ij}^{ssy} + Q\sigma_y\delta_{ij} \qquad (1)$$

where σ_{ij} is the stress field close to the crack tip of interest, σ_{ij}^{ssy} denotes the stress field under small-scale yielding conditions, σ_y is the yield stress and δ_{ij} is Kronecker's delta. Whilst Q may vary slightly with distance from the

crack tip, r, it is conventionally defined at a fixed normalised distance $r\sigma_y/J=2$ directly ahead of the crack, where J is the J-integral.

These developments have coincided with advances in the use of miniature specimens. Whilst testing standards provide limits on specimen sizes for the measurement of toughness in many practical situations the limited availability of material means that it is impractical to test sufficiently large specimens to generate valid toughness data. As a result, a number of experimental programmes have sought to relate 'invalid' data derived from miniature specimens to 'valid' data via scaling laws, e.g. [2].

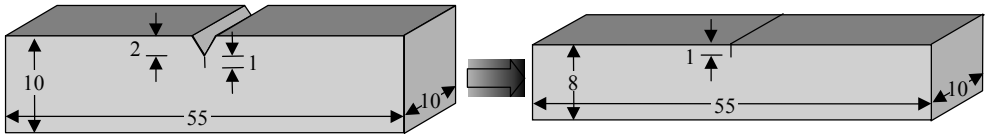

Figure 1: Geometry of PC-CVN and modified 3PB specimens

The current work has brought these two areas together to evaluate the use of miniature specimens to derive low constraint cleavage toughness data. A pre-cracked Charpy V-notch (PC-CVN) test piece has been used to develop a shallow-cracked three-point bend (3PB) specimen, Figure 1. Three-dimensional finite element analyses (FEA) have quantified $K_J=(E'J)^{0.5}$, where J is the J-integral, $E'=E/(1-\nu^2)$ in plane strain, E being Young's modulus and ν Poisson's ratio, and Q across the crack front. Experimental work has provided practical experience to evaluate this specimen.

MATERIAL

The material used in this study is the A508 Class 3 steel used within the NESC-I programme [3]. Tensile properties at ambient temperature are summarised in Table 1. Fracture toughness properties may be described by a Master Curve [2] with reference temperature T_0 equal to 68ºC and 32ºC for high and low constraint specimens, respectively [3].

TABLE 1: Mechanical properties of A508-3 steel

Temperature (ºC)	Young's modulus (MPa)	Yield stress (MPa)
20	220,000	570

INITIAL CONSIDERATIONS

In order to evaluate the suitability of the 3PB specimen shown in Figure 1 to derive low constraint toughness, limit load, constraint and pre-cracking issues were initially considered. The von Mises plane strain limit load (P_L) for a shallow-cracked 3PB geometry is given by [4]:

$$P_L = 1.210\ \sigma_y\ W^2\ B\ \gamma\ (1\text{-}a/W)^2/2L \quad \text{for } a/W < 0.177 \qquad (2)$$

where, W is the specimen width, B is the thickness, 2L is the span, a is the crack length and $\gamma=2/\sqrt{3}$. At 20ºC, P_L=9.7kN.

The Q-stress for the specimen is -1.0 at K_J=150MPa$\sqrt{m}$ assuming a power-law hardening exponent n=10 [1]. The Q-stress is defined more precisely using the results of 3D FEA in the following section.

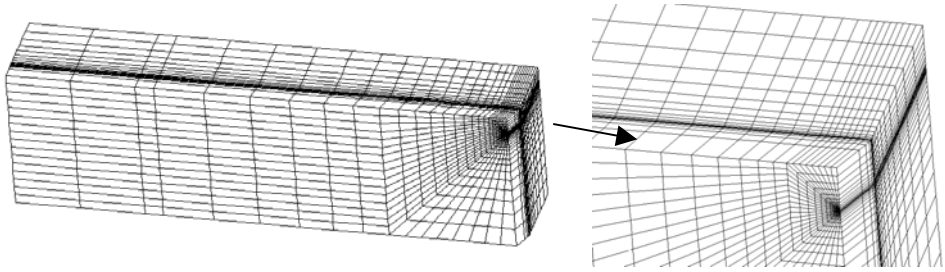

Figure 2: Finite element model of 3PB specimen with 20% side-grooves

Fatigue pre-cracking of Charpy specimens may be performed under cyclic bending from the existing V-notch. Specimens may be pre-cracked at a maximum K = 25 to 30MPa$\sqrt{m}$ at a frequency of approximately 100Hz. The loads required are less than half the limit load.

FINITE ELEMENT ANALYSES

Two 3D models were developed to simulate side-grooved and non side-grooved 3PB specimens. Each model represented one quarter of the specimen with appropriate boundary conditions applied to nodes situated on the two symmetry planes. The side-grooved model, Figure 2, consisted of 13,824 eight-noded full integration elements arranged into variable thickness planar layers. Loading was simulated via a pressure applied to the top surface of thin elements located on the upper surface of the model,

coincident with the loading point on the test specimen. The nodes located on the back face directly ahead of the crack-tip were fully constrained.

Figures 3(a-d) illustrate the variation of K_J, and Q along the crack front for plane and 20% side-grooved specimens. K_J was derived from the J-integral assuming plane-strain conditions. Since K_J is dependent on the position (z) along the crack front, it is denoted K_z. Similarly Q, derived from the hydrostatic stress field according to Eqn. (1), is denoted Q_z. Results are presented at four values of the average crack driving force, K_{ave}, calculated using a weighted average. An average Q-stress, Q_{ave}, was derived in a similar manner.

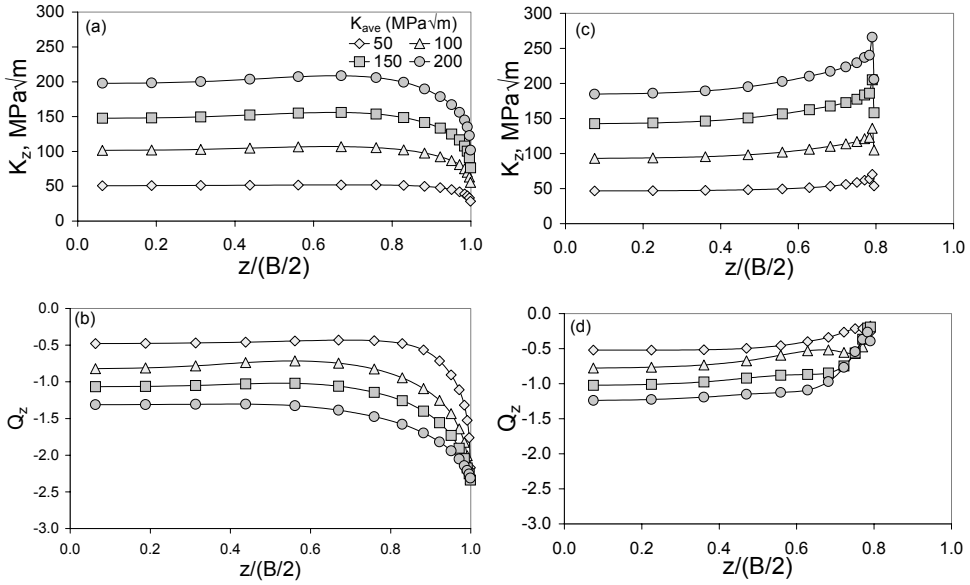

Figure 3: FEA results for plane specimens (a) K_z and (b) Q_z and side grooved specimens (c) K_z and (d) Q_z

For plane specimens, Figure 3(a), the maximum crack driving force is located within the body of the specimen at z/(B/2)=0.65, with K_J decreasing towards the outside surface, z=(B/2). For K_{ave}=50MPa√m, K_z is approximately constant over ~90% of the crack front. With increasing load, the percentage of crack front under a constant K_z remains broadly constant.

For side-grooved 3PB specimens, Figure 3(c), the peak crack driving force is located towards the root of the side-groove and reduces towards the centre of the specimen. The value of K_z at the side-groove is of the order of 25 % higher than at the centre of the specimen.

The variation of Q-stress across the crack front mirrors the variation of K_J. For plane specimens, Q_z is a maximum over the central region of the specimen, whilst for side-grooved specimens, it peaks towards the root of the side-groove. This is likely to be caused by the local stress concentrating effect of the side-groove increasing stress triaxiality in this region. For plane and side-grooved 3PB specimens, Figures 3(b) and 3(d) respectively, Q_z is approximately equal to –0.5 at the centre of the specimen for K_{ave}=50MPa√m. For K_{ave}=150MPa√m, Q_z reduces to approximately –1.25.

Figure 4 illustrates the variation of K_{ave} versus Q_{ave} for plane and side-grooved specimens. At K_{ave}=150MPa√m Q_{ave} is equal to –1.15 and –0.86 for plane and side-grooved specimens, respectively.

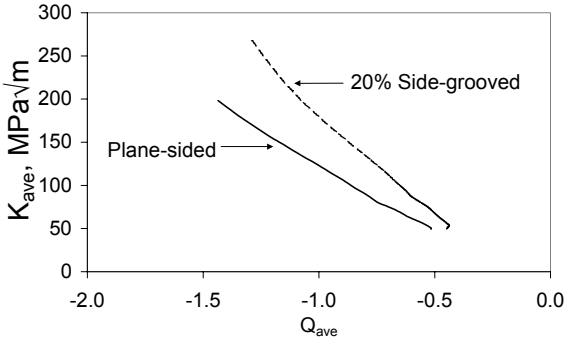

Figure 4: Variation of K_{ave} with Q_{ave} for plane and side-grooved specimens

EXPERIMENTAL

Fifteen CVN specimens (designated VL1 to VL15) were pre-cracked under cyclic three-point bending, at an initial maximum stress intensity factor of 27MPa√m, reducing to 25MPa√m, at a frequency of approximately 100Hz. The minimum to maximum applied stress ratio was 0.1. Pre-cracks extended approximately 1mm below the V-notch.

The upper 1.8mm of each specimen was subsequently removed by milling and the final 0.2mm was removed by grinding to +/- 0.05mm. This produced specimens of width W=8mm and initial crack depth $a_0 \approx 1$mm.

Specimens were tested in displacement control under three-point bending with an outer span of 40mm at a loading rate of ~0.05mm/min at ambient temperature. Applied load and load-line displacement were monitored up to specimen failure, which was by brittle cleavage in all cases.

Fracture surfaces were examined under an optical microscope to assess whether cleavage fracture was preceded by any ductile crack extension. In all but two cases, the amount of pre-cleavage tearing (defined by a nine-point average) was less than 0.1mm. Such a small level of extension is likely to be associated with crack blunting, rather than with ductile tearing.

Fracture toughness was derived from the load-displacement traces according to a partitioned J:

$$J = \frac{K^2\left(1-\nu^2\right)}{E} + \frac{\eta_p U_p}{B\left(W-a\right)} \tag{3}$$

where U_p is the plastic area under the load versus load-point displacement trace and η_p is given by [5]:

$$\eta_p = 0.32 + 12(a/W) - 49.5(a/W)^2 + 99.8\,(a/W)^3 \tag{4}$$

In each case, the measured load versus load-line displacement data were corrected for indentation by aligning the elastic portion of the trace to the theoretical compliance.

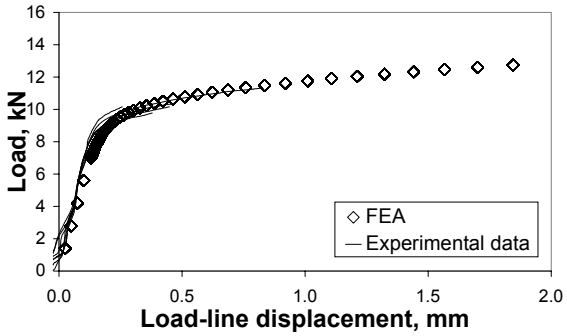

Figure 5: Load-displacement behaviour

RESULTS AND DISCUSSION

Experimental load-displacement traces are compared with the FEA prediction in Figure 5. Good agreement is obtained. Resultant fracture toughness data are compared with high and low constraint data obtained within the NESC programme in Figure 6. The data are higher than both

high and low constraint curves obtained in the NESC programme. This is probably due to the specimen geometry used in the present work, i.e. W≠B.

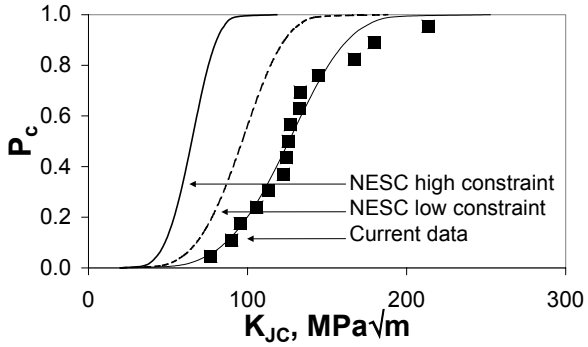

Figure 6: Fracture toughness as a function of cleavage probability

The data are plotted on an R6 Option 1 failure assessment diagram [6] in Figure 7. The material toughness, K_{mat}, has been taken as the 5% toughness from the NESC high-constraint transition curve, i.e. 43 MPa√m. The limit load has been taken as 9.7kN, derived from Eqn. (2). As expected, the raw data (closed symbols) lie outside the failure assessment curve.

The data have been "constraint-corrected" according to the constraint-based procedure II described within Section III.7 of R6 [6]. Here, K_r is defined in terms of the measured low constraint toughness $K^{\smile}_{mat}$ rather than K_{mat}. The constraint corrected data (open symbols) lie close to the failure assessment curve, providing useful validation for this procedure.

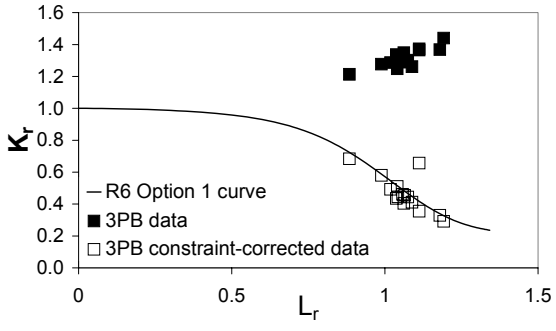

Figure 7: Fracture toughness data plotted on an R6 Option 1 diagram

CONCLUSIONS

1. Charpy V-notch test pieces may be used to produce shallow-cracked bend specimens.
2. For non-side-grooved specimens, the peak crack driving force and constraint condition is located towards the centre of the specimen. For 20% side-grooved specimens, the peak crack driving force and constraint condition is focussed towards the root of the side-groove.
3. Tests performed on shallow-cracked 3PB specimens have confirmed that this geometry may be used to generate low constraint fracture toughness data at temperatures in the lower transition regime.
4. The fracture toughness data obtained in this study are higher than those generated in the NESC project for deep and shallow cracked specimens.
5. The data provide validation for the constraint-based methods within the R6 procedure.

ACKNOWLEDGEMENTS

This work was carried out within the R6 Development Programme co-ordinated by British Energy Generation Ltd. The paper is published with the permission of Serco Assurance and British Energy Generation Ltd.

REFERENCES

1. N P O'Dowd (1995) "Applications of two-parameter approaches in elastic-plastic fracture mechanics", *Engng Frac. Mech.*, **52**, pp.445-465.
2. K Wallin, T Planman, M Valo and R Rintamaa (2001) "Applicability of miniature sized bend specimens to determine the Master Curve reference temperature, T_0"*Eng. Frac. Mech*., **68**, pp.1265-1296.
3. R Bass, J Wintle and R C Hurst (2001), "NESC-I Project Overview", EUR 19051EN, published by the European Communities.
4. G A Webster and R A Ainsworth (1994) "High temperature component life assessment", Chapman and Hall.
5. J D G Sumpter and J W Hancock (1994) "A Status Review of the J plus T stress Fracture Analysis Method", 6th European Conference on Fracture: Structural Integrity - Experiments Models and Applications published by EMAS Warley ISBN 0 947817 73 5
6. British Energy Generation Limited (2001) "Assessment of the Integrity of Structures Containing Defects", R/H/R6 – Revision 4.